(*E*)-4-Aryl-4-oxo-2-butenoic Acid Amides, the Chalcone-Aroylacrylic Acid Chimeras. Design, Antiproliferative Activity and Inhibition of Tubulin Polymerization

Maja D. Vitorovic-Todorović,[*] Aleksandra Erić, Branka Kolundžija, Ernest Hamel, Slavica Ristić, Ivan O. Juranić, Branko J. Drakulić

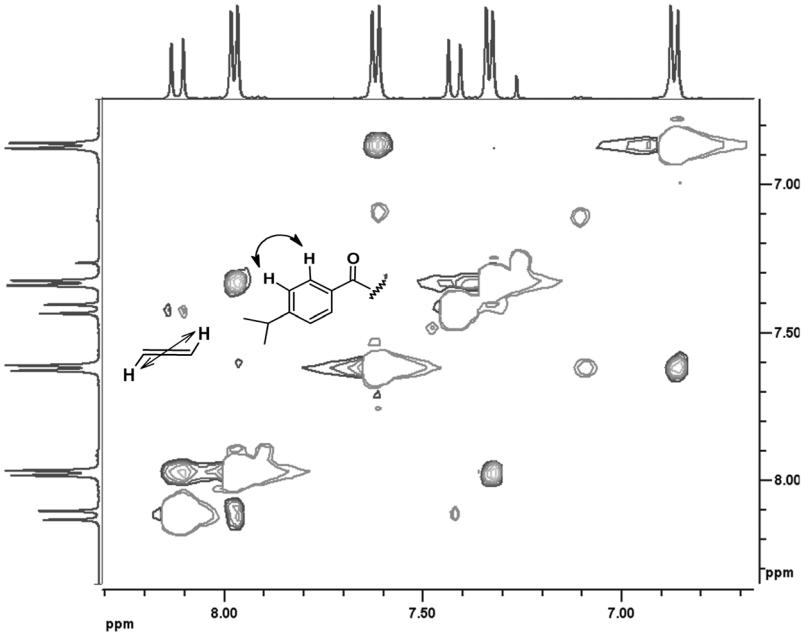

Figure S1. NOESY signals between -CH=CH- protons, and between *ortho*- and *meta*- protons on aryl ring of derivative **11**.

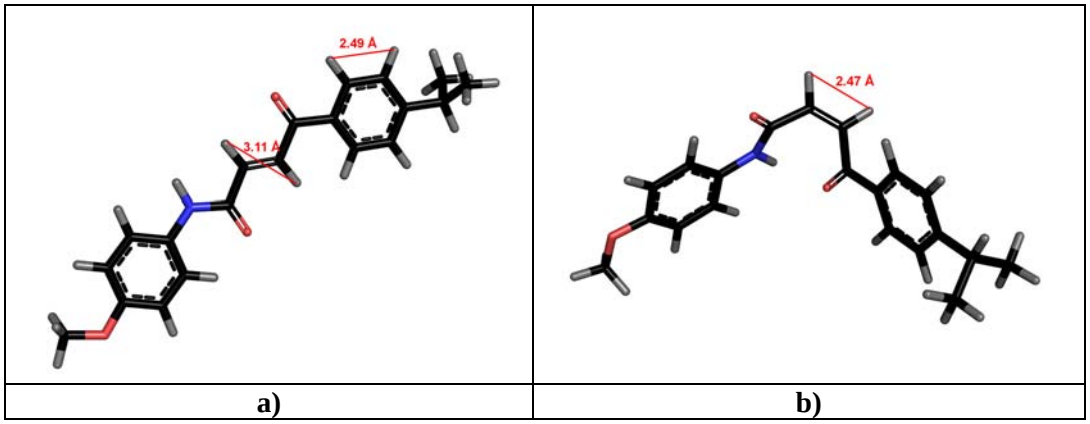

Figure S2. Optimized geometries of derivative **11** in it's a) (*E*)-, and b) (*Z*)-form.

[*] Correspond to: mvitod@chem.bg.ac.rs

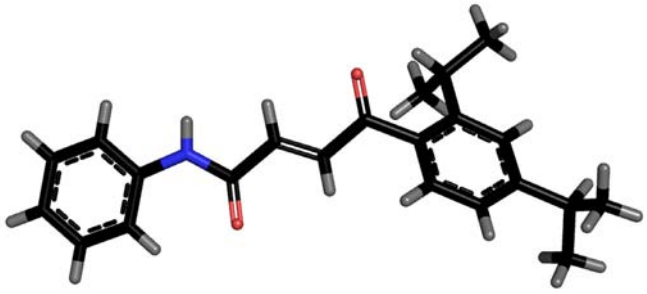

Figure S3. Geometry of derivative **12**, as obtained by single-crystal x-ray analysis.

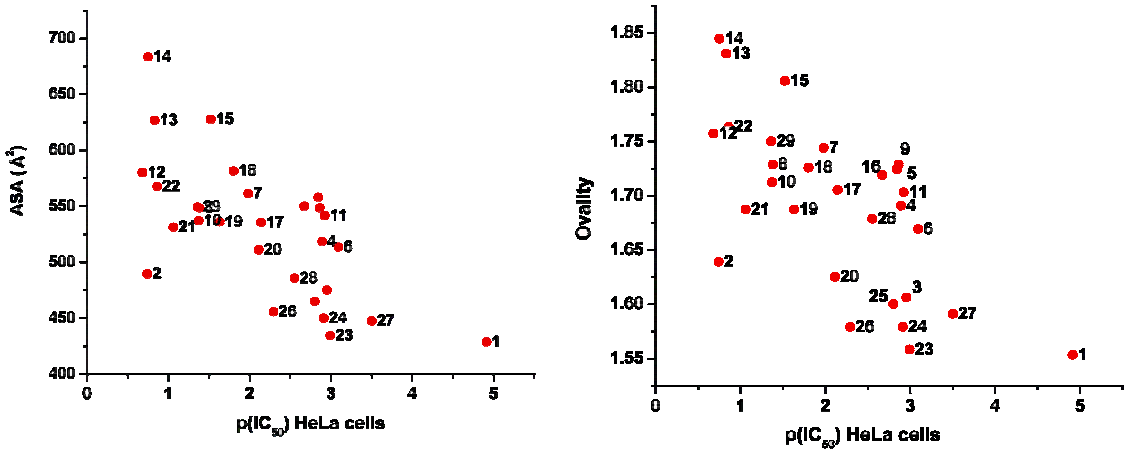

a) **b)**

Figure S4. Trend between p(IC_{50}) toward HeLa cells and a) apolar surface area, and b) ovality of compounds **1**-**29**.

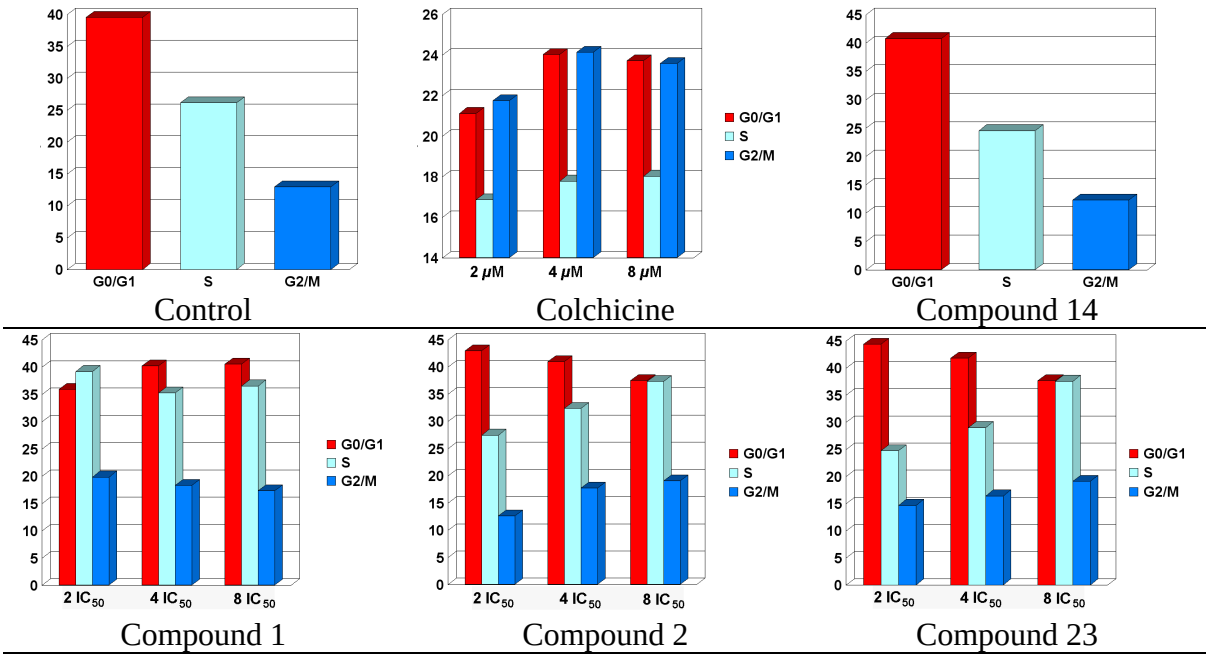

Figure S5. Cell cycle analysis of compounds **1**, **2**, **14** and **23**, Table 3 in the main text.

Table S6. Some 3D-dependant properties of **1**-**29**, for conformations obtained as energy minima by OMEGA and MMFF94s.

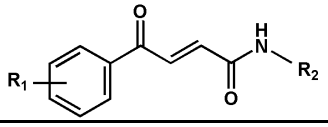

	R_1-	R_2-	Solvent Accessible Area	Apolar Surface Area	Volume	Ovality	Vlog*P*
1[*]	H	Ph-	509.9	428.9	235.5	1.5535	2.1945
2[*]	2,5-di-Me	Ph-	569.9	489.7	263.0	1.6393	3.0778
3[*]	3,4-di-Me	Ph-	554.8	475.2	267.1	1.6063	2.9708
4	3,4-di-Me	3,5-di-OMe-Ph-	633.3	518.6	316.4	1.6909	3.1674
5	3,4-di-Me	4-*i*-Pr-Ph-	637.9	558.2	315.2	1.7245	4.0284
6[*]	4-*i*-Pr	Ph-	591.7	513.6	288.1	1.6694	3.2755
7	4-*i*-Pr	3,5-di-OMe-Ph-	676.1	561.4	332.6	1.7442	3.5008
8	4-*i*-Pr	Ch-	621.6	548.6	303.5	1.7289	3.4775
9[*]	2,5-di-Me	Bn-	621.6	548.6	303.5	1.7289	3.4775
10[#]	4-*i*-Pr	Bn-	623.6	537.2	301.6	1.7127	2.9966
11	4-*i*-Pr	4-OMe-Ph-	640.6	541.8	309.4	1.7034	3.4143
12	2,4-di-*i*-Pr	Ph-	653.4	580.2	333.1	1.7575	4.2303
13	2,4-di-*i*-Pr	3,5-di-OMe-Ph-	733.3	626.9	385.3	1.8311	4.5257
14	2,4-di-*i*-Pr	4-*i*-Pr	754.1	683.7	383.7	1.8449	5.3879
15	2,4-di-*i*-Pr	Bn-	702.7	627.8	346.4	1.8059	4.1541
16	*β*-tetralinoyl	3,5-di-OMe-Ph-	660.9	550.1	339.6	1.7192	3.7478
17[*]	*β*-tetralinoyl	Ch-	603.5	535.7	305.0	1.7055	3.7381
18	*β*-tetralinoyl	4-i-Pr-Ph-	658.8	581.7	341.6	1.7261	4.4992
19[#]	*β*-tetralinoyl	Bn-	618.6	536.2	307.8	1.6875	3.4062
20[*]	*β*-tetralinoyl	Ph-	595.2	511.2	287.9	1.6254	3.4416
21[*]	4-*n*-Bu	Ph-	609.3	531.4	301.3	1.6875	3.1340
22	2,3,5,6-tetra-Me	3,5-di-OMe-Ph-	678.6	567.8	348.6	1.7637	4.0446
23[*]	4-F	Ph-	514.2	434.5	239.0	1.5584	2.4130
24[*]	4-Cl	Ph-	529.7	450.1	247.0	1.5793	2.8163
25[*]	3,4-di-Cl	Ph-	544.8	465.2	260.2	1.6003	3.3713
26[*]	4-Br	Ph-	535.5	455.9	252.1	1.5792	3.0228
27[*]	4-OMe	Ph-	547.1	447.6	259.1	1.5912	2.3008
28	4-OMe	3,5-di-OMe-Ph-	620.3	485.8	308.1	1.6789	2.4709
29	3,5-di-Me-4-OMe	3,5-di-OMe-Ph-	675.7	549.4	335.2	1.7503	3.3902

[*]Inhibited tubulin assembly with IC_{50} values < 20 μM; [#] **19** has a SAS, and **10** has a volume somewhat below cut-offs, as described in the text, and did not inhibit tubulin assembly with IC_{50} values < 20 μM.

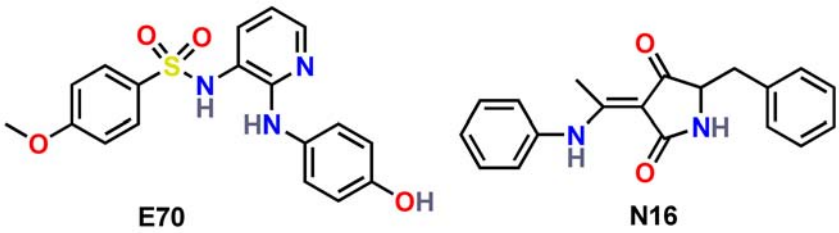

Scheme S7. 2D structures of E70 and N16.

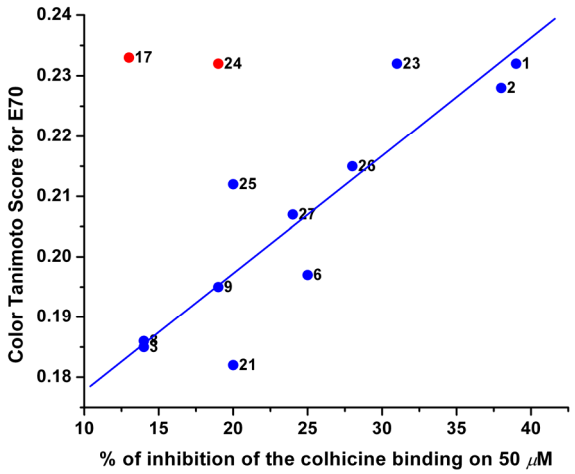

Figure S8. Trend between the percentage of inhibition of colchicine binding at 50 μM and the pharmacophoric similarity of compounds with E70.

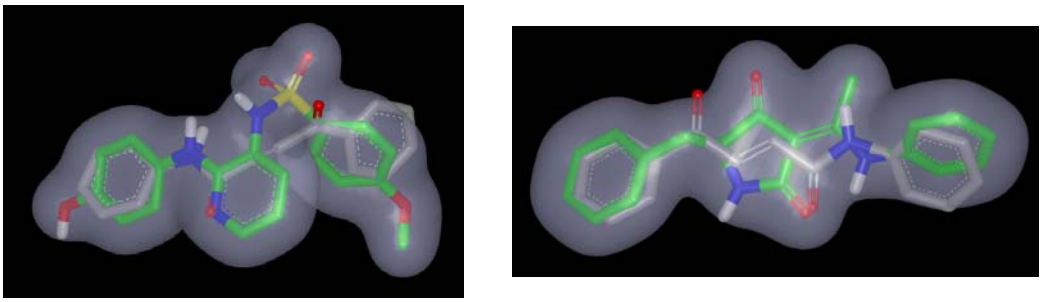

1 *vs* E70, TC = 0.85 **1** *vs* N16, TC = 1.03

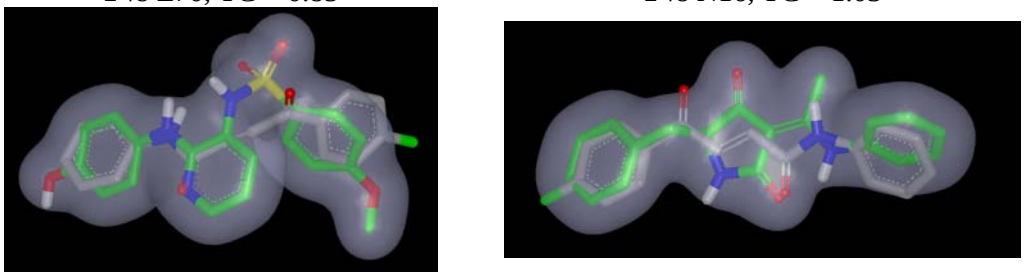

23 *vs* E70, TC = 0.83 **23** *vs* N16, TC = 1.05

Figure S9. Compounds **1** and **23** overlapped on E70 and N16. Similarity obtained by Tanimoto combo (TC) scoring.